

Received August 7, 2021, accepted August 18, 2021, date of publication August 24, 2021, date of current version October 1, 2021.

Digital Object Identifier 10.1109/ACCESS.2021.3107537

Compact TSV-Based Hairpin Bandpass Filter for Thz Applications

FENGJUAN WANG¹, (Member, IEEE), LEI KE¹, XIANGKUN YIN²,
NINGMEI YU¹, (Member, IEEE), AND YUAN YANG¹

¹School of Automation and Information Engineering, Xi'an University of Technology, Xi'an 710048, China

²School of Microelectronics, Xidian University, Xi'an, Shaanxi 710071, China

Corresponding author: Xiangkun Yin (yinxkc@163.com)

This work was supported in part by the National Natural Science Foundation of China under Grant 61774127, Grant 61804112, Grant 61771388, and Grant 62174134; in part by FokYing Tung Education Foundation under Grant 171112; in part by Shaanxi Innovation Capacity Support Project under Grant 2020KJXX-093 and Grant 2021TD-25; in part by Shaanxi Provincial Education Department Youth Innovation Team Construction Research Program under Grant 21JP080; in part by The Fundamental Research Funds for the Central Universities under Grant JB211110.

ABSTRACT A hairpin bandpass filter with compact feeder structure is proposed for terahertz (THz) applications by using the model of odd-even propagation mode. By employing the three-dimensional integrated through-silicon via (TSV) technology, the proposed filter exhibits an ultra-compact size of only $0.24 \times 0.028 \text{ mm}^2$ ($1.38 \times 0.16 \lambda_g^2$). The model of the proposed filter is established and optimized with the HFSS tool based on finite element method. The results of S -parameters reveal that the proposed filter with center frequency at 0.5 THz, exhibits a bandwidth of 0.08 THz with insertion loss of 1.5 dB and reflection loss over 13.4 dB in the passband.

INDEX TERMS Hairpin bandpass filter, terahertz applications, odd-even model, through-silicon via (TSV).

I. INTRODUCTION

The filter is the most important component for the radio-frequency (RF) communication front end [1]–[4]. A hairpin filter with resonators is the simplest structure used for microstrip filters exhibiting the appealing features of miniaturization, easy integration, and high-gain [5]–[13]. Presently, a great deal of researches on hairpin filters focus on microstrip planar hairpin units [5]–[16]. However, the microstrip line structure fails to operate normally at above 0.1 THz frequency due to excessive losses.

Fortunately, the through-silicon via (TSV) technology has been shown to be a good candidate for miniaturization and integration of passive devices [17]–[24]. TSV is a vital component of 3-D ICs [25], [26], [29], [32], which can extend Moore's law for several more technology nodes despite the bottleneck of physical size transistor scaling [29]. Based on these observations, a TSV-based hairpin bandpass filter has been proposed as a well-suited component for THz applications. However, this filter exhibits insertion loss of as much as 6.9 dB and, therefore, does not satisfy the basic performance index of the filter. The structure of hairpin filter needs to be more improved for operating at the THz frequency range.

The associate editor coordinating the review of this manuscript and approving it for publication was Wen-Sheng Zhao¹.

In this paper, a compact TSV-based hairpin bandpass filter for THz applications is proposed. In addition, as the traditional design method of the hairpin filter is based on microstrip structure in frequencies lower than THz, there is no prior work investigating the behavior and design process for TSV-based hairpin filters in THz band. To fill this gap, this paper proposes to design hairpin filter based on TSV in THz band following a structure that cannot be supported by traditional microstrip structures that incur considerably overhead in area and form factors.

This paper is organized as follows. The design method of the proposed filter with TSV and compact feeder is described in Section II. The results and a discussion around the S -parameter curves are presented in Section III. Conclusions are drawn in Section IV.

II. DESIGN OF TSV-BASED HAIRPIN BANDPASS FILTER

The proposed filter is based on the Chebyshev filter, adopting TSV and tailoring the feeder position to THz applications. The filtering function of the proposed filter is realized by the coupling action between hairpin units, which can be analyzed by using odd-even model. Each hairpin unit consists of two through-silicon vias (TSVs) as arms and one RDL segment as connection. The input-output feeder with compact size is the interface between the power supply and the proposed filter.

The proposed methodology is also applicable to other filters based on this geometry.

A. COMPACT FEEDER

The input and output design includes the same three parts, which are the TSV, RDL segment, and feeder described in Fig. 1.

The TSV has diameter D and length L_2 , respectively. The RDL segment has length L_3 , width W , and height H_2 . Furthermore, the feeder has length L_1 , width W , and height H_1 . The feeder of hairpin filter is designed to obtain the maximum transmission efficiency. The feeder is a branch modulator that matches the impedance of the filter. As depicted in Fig. 1, l is the distance from the middle of RDL to the middle of feeder, while L is the distance from the middle of RDL to the top of TSV.

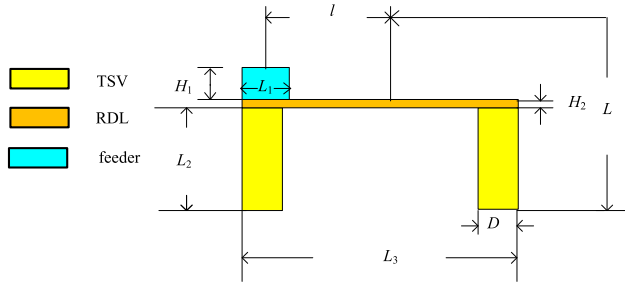


FIGURE 1. The structure of input design in hairpin filter and the related design parameters.

The ratio of l to L is related to the effect of impedance matching. There is a theoretical relation between l to L [27] given by

$$l = \frac{2L}{\pi} \cdot \arcsin \sqrt{\frac{\pi R}{2Z_0 Q_{e1}}}, \quad (1)$$

where R and Z_0 are the characteristic impedances of feeder and hairpin unit, respectively. These impedances have the same value of 50Ω . Q_{e1} is external coupling coefficient, which can be obtained from [28]

$$Q_{e1} = \frac{g_0 g_1}{(\omega_{p2} - \omega_{p1}) / \sqrt{\omega_{p2} \omega_{p1}}}, \quad (2)$$

where g_0 and g_1 can be obtained by the Chebyshev low pass filter element table [30]. ω_{p1} and ω_{p2} are, respectively, the predesigned lower passband frequency and upper passband frequency.

In this paper, l is made up of $0.5 W_1$, W and $0.5 L_3$, while L is made up of L_2 , W and $0.5 L_3$. L can be given by [6]

$$L = \frac{c}{4f_0 \sqrt{\epsilon_e}}, \quad (3)$$

$$\epsilon_e = \frac{\epsilon_r + 1}{2} + \frac{\epsilon_r - 1}{2} \left(\frac{1}{\sqrt{1 + 12 \frac{h}{W}}} \right), \quad (4)$$

$$W = \frac{8he^A}{e^{2A} - 2}, \quad (5)$$

$$A = \frac{Z_0}{60} \sqrt{\left(\frac{\epsilon_r + 1}{2} \right) + \left(\frac{\epsilon_r - 1}{\epsilon_r + 1} \right) \left(0.23 + \frac{0.11}{2} \right)}, \quad (6)$$

$$\times \left(\frac{W}{h} < 2l \right),$$

where f_0 and c are, respectively, the center frequency and the speed of light in vacuum. ϵ_0 and h are, respectively, dielectric constant and height of substrate. The substrate of the proposed filter is a high-resistance silicon substrate with a dielectric constant of 11.9, dielectric tangent of 0.005 and resistivity of $1000 \Omega \cdot \text{cm}$. In this paper, h is the distance between double conductors of the proposed filter.

L_2 as the length of TSV can be initial determined as

$$L_2 = \frac{c}{8f_0 \sqrt{\epsilon_e}}, \quad (7)$$

where ϵ_e can be obtained from Eqs.(4)-(6). In addition, L_1 as the length of feeder can be obtained from Eqs.(5)-(6).

The structure of feeder is compact due to the low height. In addition, the length of the RDL segment can be determined as

$$L_3 = 1.438 (L_2 + H_2 + 1.429L_1). \quad (8)$$

B. COUPLING OF TSV

The coupling between two types of hairpin units which comprise the length, the diameter, and the distance of adjacent TSVs in Fig. 2.

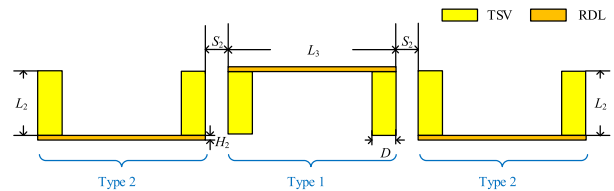


FIGURE 2. The structure of coupling of TSV in hairpin filter and the related design parameters.

As depicted in Fig. 2, S_2 is the distance between the Type 1 and Type 2 hairpin units. The impedances of adjacent TSVs can be obtained based on the impedance value analysis of odd-even propagation mode [27]. Furthermore, the diameter of TSV can be given by Eqs. (5)-(6). S_2 is inversely proportional to the coupling coefficient. The coupling coefficient is one of the decisive factors to determine the filter, which is given in theory as [28]

$$k_{i,i+1} = \frac{\omega_{p2} - \omega_{p1}}{\sqrt{\omega_{p2} \omega_{p1} g_i g_{i+1}}} \quad (i = 1, 2, 3, 4), \quad (9)$$

where $k_{i,i+1}$ is the specified interstage coupling coefficient related to electromagnetic hybrid coupling.

C. THE PROPOSED TSV-BASED HAIRPIN FILTER

As depicted in Fig. 3, the hairpin units consist of the input feeder, output feeder, and hairpin coupling line. S_1 is the space between Type 1 and Type 2 hairpin units. The value of S_1 is set equal to the radius of the TSV. In addition, the value of

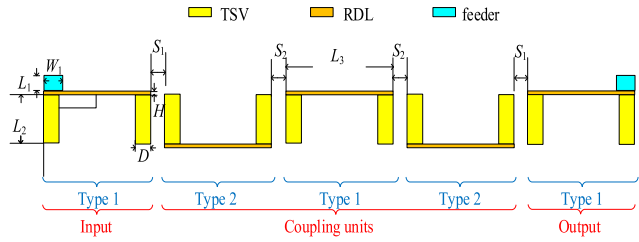


FIGURE 3. The 2D structure diagram of TSV-based hairpin bandpass filter.

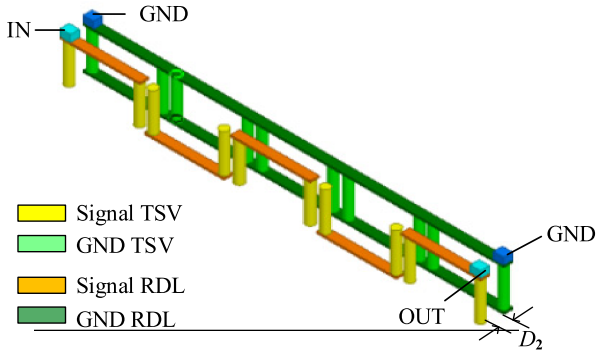


FIGURE 4. The 3D structure diagram of a TSV-based hairpin bandpass filter.

S_2 is determined by the ratio of S_2 and S_1 . In this paper, S_2 is 1.4 times as much as S_1 . For example, the value of S_2 is $7 \mu\text{m}$ while the value of S_1 is $5 \mu\text{m}$.

The distance between the ground plane and the hairpin units is D_2 , illustrated in Fig. 4. D_2 can be on the order of the dielectric layer thickness of the microstrip filter.

III. RESULTS AND DISCUSSION

The proposed filter is verified by the HFSS software and a comparison with prior THz filters is presented in this section. HFSS is used to verify the S -parameters in microwave frequencies, due to the high precision of HFSS [17], [32].

A. RESULTS

The physical size of the filter can be obtained following the design method presented in Section II.

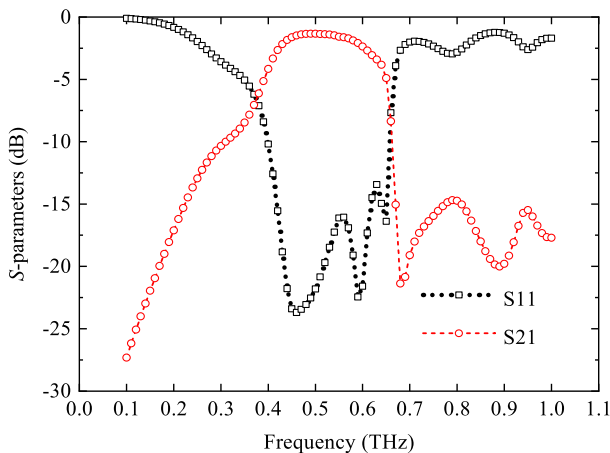


FIGURE 5. S-parameters of the proposed filter.

The TSV has D of $5 \mu\text{m}$ and L_2 of $22 \mu\text{m}$, respectively. The RDL segment has L_3 of $45 \mu\text{m}$, W of $5 \mu\text{m}$, and H_2 of $1 \mu\text{m}$. Furthermore, the feeder has L_1 of $5.8 \mu\text{m}$, W of $5 \mu\text{m}$, and H_1 of $4 \mu\text{m}$. The distances between the Type 1 and Type 2 hairpin units are S_1 of $2.5 \mu\text{m}$ and S_2 of $3.5 \mu\text{m}$. In addition, the distance between the ground plane and the hairpin units is D_2 of $8 \mu\text{m}$.

The S -parameter curves are the simulation results of the proposed filter, which are depicted in Fig. 5. It is shown that the proposed filter with center frequency at 0.5 THz , exhibits a bandwidth of 0.08 THz with insertion loss of 1.5 dB and reflection loss over 13.4 dB in the passband.

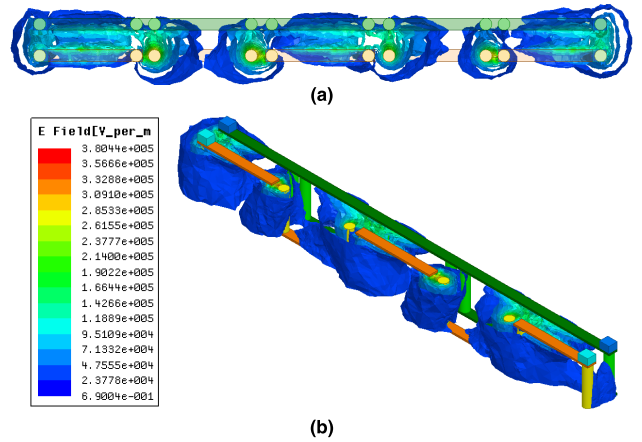


FIGURE 6. a) 2D and b) 3D E field of the proposed hairpin filter.

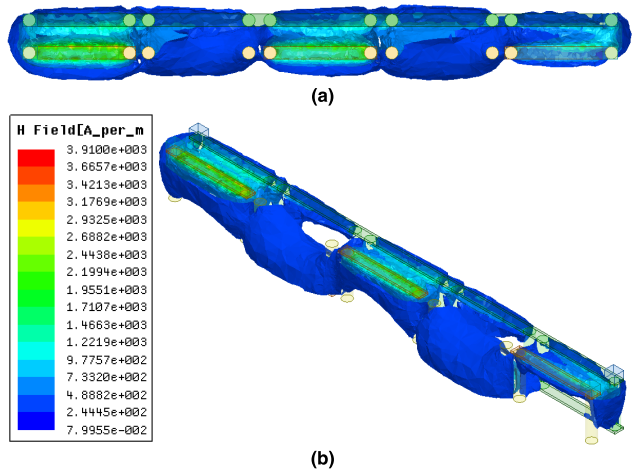


FIGURE 7. a) 2D and b) 3D H field of the proposed hairpin filter.

And the E field and H field of the proposed hairpin filter are presented in Fig. 6 and Fig. 7, which show the coupling paths. After the signal passes through the Type 1 hairpin unit and Type 2 hairpin unit, the signal phase is opposite and the energy is offset, thus generating transmission zeros. The coupling path consists of input, coupling units, and output, which are five hairpin units to transmit a quasi - TEM mode.

The proposed filter adopts direct-coupled mode, which consists of three Type 1 hairpin units and two Type 2 hairpin

units. Each Type 1 hairpin unit structure can implement the circuit function of a series connection between an inductor and a capacitor, while each Type 2 hairpin unit structure can implement the circuit function of an inductor and a capacitor in parallel. The five hairpin units realize the topological circuit with five-order coupling.

A comparison among the proposed filter and four related THz filters is performed in Table 1. Due to the introduction of TSV, the proposed filter exhibits a better coupling effect than the other filters. The 0.08 THz bandwidth of the proposed filter (listed in the fourth column of Table 1) is about 2.67×, 4.00×, 3.48×, and 1.57× higher as compared to the THz filters presented in [25], [26], [31], and [32], respectively. The size of the four related THz filters (listed in the last two columns of Table 1) is, respectively, about 8.93× [25], 87.1× [26], 211.6× [31] and 21.3× [32] greater than this work.

Because the proposed filter adopts a compact feeder structure, the size of the proposed filter is greatly miniaturized. Consequently, it can be concluded that the proposed filter has excellent performance and extremely low form factor.

TABLE 1. The comparison of the THz filters.

Filters	Type	Method	CF (THz)	BW (THz)	IL (dB)	RL (dB)	Size	
							(mm ²)	λ_g^2
[25]	Hairpin	Sim.	0.125	0.03	6.9	8	0.3×0.2	0.43×0.29
[26]	SIW	Sim.	0.16	0.02	1.5	10	0.9×0.325	2.25×0.81
[31]	SIW	Meas.	0.14	0.023	2.4	11	1.8×0.79	2.90×1.27
[32]	SIW	Meas.	0.331	0.051	1.5	15	0.68×0.21	2.60×0.80
This work	Hairpin	Sim.	0.5	0.08	1.5	13.4	0.24×0.028	1.38×0.16

B. DISCUSSION

In order to investigate the association between parameters of TSV and the performance of the proposed filter, two another comparison about three groups of D , three groups of L_2 , and three groups of L_3 (based on L_2 groups) are presented in Fig. 8, Fig. 9, and Fig. 10, respectively.

As depicted in Fig. 8, the sizes of D are 5 μm , 10 μm , and 15 μm , respectively, while the other physical size are constant. It is shown that the filter with D of 10 μm has the bandwidth of 0.1305 THz with insertion loss of 1.5 dB and reflection loss over 14.4 dB in the passband, while the filter with D of 15 μm has the bandwidth of 0.134 THz with insertion loss of 1.5 dB and reflection loss over 15.9 dB in the passband. Compare the three S -parameter curves in Fig. 8, it can be easily concluded that the in-band performance would increase a little as D increases, meanwhile the bandwidth increase.

Fig. 9 gives the S -parameters as L_2 are 22 μm , 27 μm , and 32 μm , respectively, while the other physical size are constant. It can be shown that the center frequency decreases as the L_2 of TSV increases, while the in-band performance decreases a lot. It is speculated that the performance loss

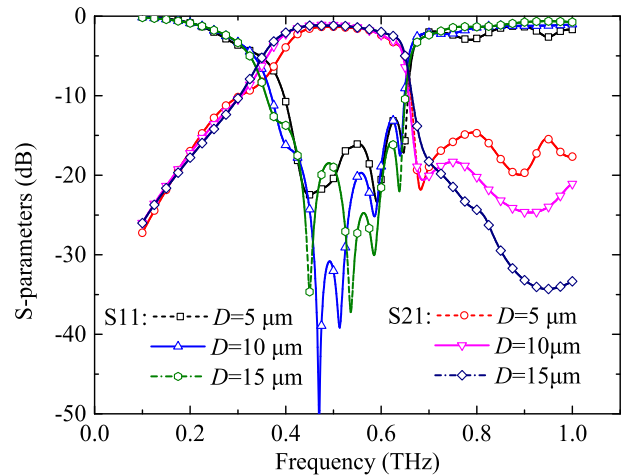


FIGURE 8. S-parameters vs. different D .

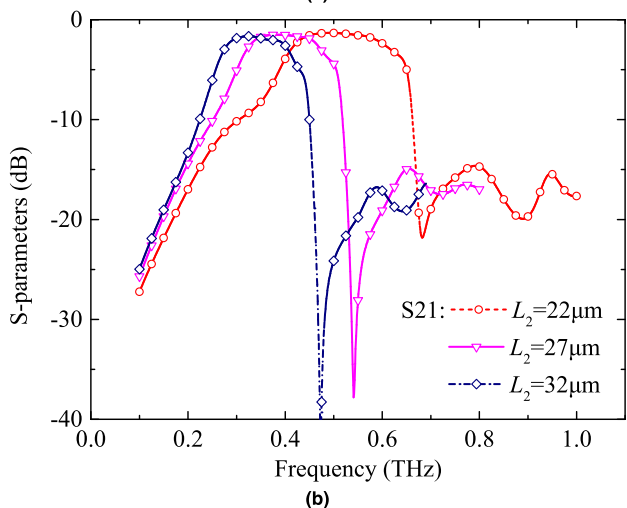
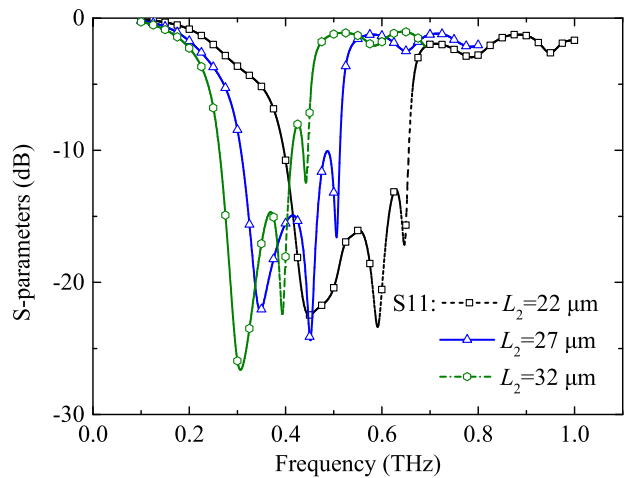


FIGURE 9. S-parameters vs. different L_2 .

reason is that the physical size of the proposed filter in Fig. 9 is not in accordance with the impedance matching characteristics.

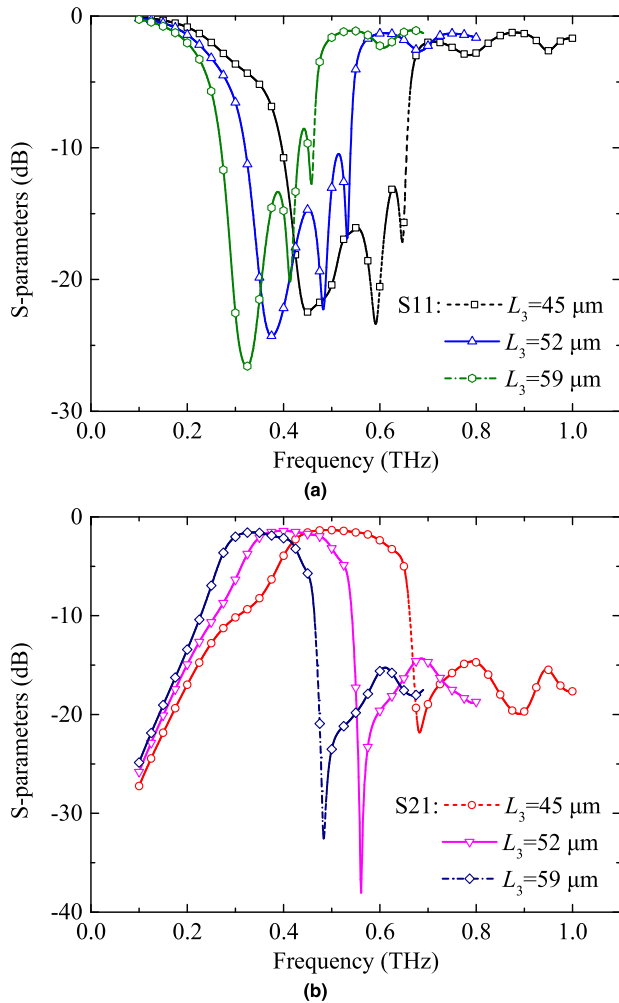


FIGURE 10. S-parameters vs. different L_3 .

As depicted in Fig. 10, the simulation results of the proposed filter with of L_3 of $45\ \mu\text{m}$, $52\ \mu\text{m}$, and $59\ \mu\text{m}$, respectively, while the other physical size are constant. Compared to the S -parameters curves in Fig. 9, the in-band performance improves a lot, because L_3 is adjusted as L_2 increases according to Eq. (8) for impedance matching.

IV. CONCLUSION

A compact TSV-based hairpin bandpass filter for THz applications is proposed and verified in the paper. The proposed filter exhibits 0.08 THz bandwidth at 0.5 THz center frequency, which can provide unprecedented data transmission rate and channel capacity for future mobile communication systems.

REFERENCES

- [1] H. Elayan, O. Amin, B. Shihada, R. M. Shubair, and M.-S. Alouini, "Terahertz band: The last piece of RF spectrum puzzle for communication systems," *IEEE Open J. Commun. Soc.*, vol. 1, pp. 1–32, 2020, doi: [10.1109/OJCOMS.2019.2953633](https://doi.org/10.1109/OJCOMS.2019.2953633).
- [2] R. Xu, S. Gao, B. S. Izquierdo, C. Gu, P. Reynaert, A. Standaert, G. J. Gibbons, W. Bosch, M. E. Gadringer, and D. Li, "A review of broadband low-cost and high-gain low-terahertz antennas for wireless communications applications," *IEEE Access*, vol. 8, pp. 57615–57629, 2020, doi: [10.1109/ACCESS.2020.2981393](https://doi.org/10.1109/ACCESS.2020.2981393).
- [3] A. Iqbal, J. J. Tiang, C. K. Lee, N. K. Mallat, and S. W. Wong, "Dual-band half mode substrate integrated waveguide filter with independently tunable bands," *IEEE Trans. Circuits Syst. II, Exp. Briefs*, vol. 67, no. 2, pp. 285–289, Feb. 2020, doi: [10.1109/TCSII.2019.2911014](https://doi.org/10.1109/TCSII.2019.2911014).
- [4] A. Zakharov, S. Litvintsev, and M. Ilchenko, "Transmission line tunable resonators with intersecting resonance regions," *IEEE Trans. Circuits Syst. II, Exp. Briefs*, vol. 67, no. 4, pp. 660–664, Apr. 2020, doi: [10.1109/TCSII.2019.2922429](https://doi.org/10.1109/TCSII.2019.2922429).
- [5] M. F. Haider, F. You, T. Qi, and W. Shi, "A 10W broadband power amplifier with a hairpin resonator filter based on even-odd mode impedance analysis," in *Proc. Eur. Microw. Conf. Central Eur.*, May 2019, pp. 366–369.
- [6] M. Fadhil, H. Wijanto, and Y. Wahyu, "Hairpin line bandpass filter for 1.8 GHz FDD-LTE eNodeB receiver," in *Proc. Int. Conf. Radar, Antenna, Microw., Electron., Telecommun. (ICRAMET)*, Oct. 2017, pp. 134–136, doi: [10.1109/ICRAMET.2017.8253161](https://doi.org/10.1109/ICRAMET.2017.8253161).
- [7] N. A. Wahab, W. Norsyafizan W. Muhamad, M. M. A. M. Hamzah, S. S. Sarmin, and N. F. Naim, "Design a microstrip hairpin band-pass filter for 5GHz unlicensed Wimax," in *Proc. Int. Conf. Netw. Inf. Technol.*, Jun. 2010, pp. 183–186, doi: [10.1109/ICNIT.2010.5508533](https://doi.org/10.1109/ICNIT.2010.5508533).
- [8] J.-x. Sun, Z.-x. Huang, X.-l. Wu, H. Wang, and Y. Zhou, "Design of image-reject hairpin filter applied for Ku-band LNB," in *Proc. 9th Int. Symp. Antennas, Propag. EM Theory*, Nov. 2010, pp. 1161–1164, doi: [10.1109/ISAPE.2010.5696685](https://doi.org/10.1109/ISAPE.2010.5696685).
- [9] W. Wang, S. Yang, and Y. Chen, "Experimental design on microstrip line bandpass filters for WCDMA," in *Proc. Int. Conf. Multimedia Technol.*, Jul. 2011, pp. 3054–3057, doi: [10.1109/ICMT.2011.6001956](https://doi.org/10.1109/ICMT.2011.6001956).
- [10] T. Singh, J. Chacko, N. Sebastian, R. Thoppilan, A. Kotrashetti, and S. Mande, "Design and optimization of microstrip hairpin-line bandpass filter using DOE methodology," in *Proc. Int. Conf. Commun., Inf. Comput. Technol. (ICCICT)*, Oct. 2012, pp. 1–6, doi: [10.1109/ICCICT.2012.6398177](https://doi.org/10.1109/ICCICT.2012.6398177).
- [11] M. F. Haider, F. You, W. Shi, S. Ahmad, and T. Qi, "Broadband power amplifier using hairpin bandpass filter matching network," *Electron. Lett.*, vol. 56, no. 4, pp. 182–184, Feb. 2020, doi: [10.1049/el.2019.3047](https://doi.org/10.1049/el.2019.3047).
- [12] A. Zakharov, S. Rozenko, and M. Ilchenko, "Varactor-tuned microstrip bandpass filter with loop hairpin and combine resonators," *IEEE Trans. Circuits Syst. II, Exp. Briefs*, vol. 66, no. 6, pp. 953–957, Jun. 2019, doi: [10.1109/TCSII.2018.2873227](https://doi.org/10.1109/TCSII.2018.2873227).
- [13] H. Liu, B. Ren, S. Hu, X. Guan, P. Wen, and J. Tang, "High-order dual-band superconducting bandpass filter with controllable bandwidths and multitransmission zeros," *IEEE Trans. Microw. Theory Techn.*, vol. 65, no. 10, pp. 3813–3823, Oct. 2017, doi: [10.1109/TMTT.2017.2690295](https://doi.org/10.1109/TMTT.2017.2690295).
- [14] A. Sheikhi, A. Alipour, and A. Mir, "Design and fabrication of an ultra-wide stopband compact bandpass filter," *IEEE Trans. Circuits Syst. II, Exp. Briefs*, vol. 67, no. 2, pp. 265–269, Feb. 2020, doi: [10.1109/TCSII.2019.2907177](https://doi.org/10.1109/TCSII.2019.2907177).
- [15] V. N. R. Vanukuru and V. K. Velidi, "CMOS millimeter-wave ultra-wideband bandpass filter with three reflection-zeros using compact single TFMS coupled-line hairpin unit," *IEEE Trans. Circuits Syst. II, Exp. Briefs*, vol. 67, no. 1, pp. 77–81, Jan. 2020, doi: [10.1109/TCSII.2019.2903324](https://doi.org/10.1109/TCSII.2019.2903324).
- [16] B. Chen, Y. Tang, H. Zhu, H. Yue, Z. Wen, and X. Deng, "Design of W band hairpin filter with IPD technology," in *IEEE MTT-S Int. Microw. Symp. Dig.*, May 2019, pp. 1–3, doi: [10.1109/IEEE-IWS.2019.8804145](https://doi.org/10.1109/IEEE-IWS.2019.8804145).
- [17] X. Yin, Z. Zhu, Y. Liu, Q. Lu, X. Liu, and Y. Yang, "Ultra-compact TSV-based L-C low-pass filter with stopband up to 40 GHz for microwave application," *IEEE Trans. Microw. Theory Techn.*, vol. 67, no. 2, pp. 738–745, Feb. 2019, doi: [10.1109/TMTT.2018.2882809](https://doi.org/10.1109/TMTT.2018.2882809).
- [18] L. Qian, K. Qian, X. He, Z. Chu, Y. Ye, G. Shi, and Y. Xia, "Through-silicon via-based capacitor and its application in LDO regulator design," *IEEE Trans. Very Large Scale Integr. (VLSI) Syst.*, vol. 27, no. 8, pp. 1947–1951, Aug. 2019, doi: [10.1109/TVLSI.2019.2904200](https://doi.org/10.1109/TVLSI.2019.2904200).
- [19] J. Jeong, J.-S. Yoon, and R.-H. Baek, "Analysis of TSV-induced mechanical stress and electrical noise coupling in sub 5-nm node nanosheet FETs for heterogeneous 3D-ICs," *IEEE Access*, vol. 9, pp. 16728–16735, 2021, doi: [10.1109/ACCESS.2021.3053572](https://doi.org/10.1109/ACCESS.2021.3053572).
- [20] X. Yin, Z. Zhu, Y. Yang, and R. Ding, "Metal proportion optimization of annular through-silicon via considering temperature and keep-out zone," *IEEE Trans. Compon., Packag., Manuf. Technol.*, vol. 5, no. 8, pp. 1093–1099, Aug. 2015, doi: [10.1109/TCPMT.2015.2446768](https://doi.org/10.1109/TCPMT.2015.2446768).
- [21] V. F. Pavlidis, I. Savidis, and E. G. Friedman, *Three-Dimensional Integr. Circuits Design*, 2nd ed. Amsterdam, The Netherlands: Elsevier, 2017.

- [22] K. N. Dang, A. B. Ahmed, A. B. Abdallah, and X.-T. Tran, "A thermal-aware on-line fault tolerance method for TSV lifetime reliability in 3D-NoC systems," *IEEE Access*, vol. 8, pp. 166642–166657, 2020, doi: [10.1109/ACCESS.2020.3022904](https://doi.org/10.1109/ACCESS.2020.3022904).
- [23] X. Yin, Z. Zhu, Y. Yang, and R. Ding, "Effectiveness of $p+$ layer in mitigating substrate noise induced by through-silicon via for microwave applications," *IEEE Microw. Wireless Compon. Lett.*, vol. 26, no. 9, pp. 687–689, Sep. 2016, doi: [10.1109/LMWC.2016.2597218](https://doi.org/10.1109/LMWC.2016.2597218).
- [24] Q. Lu, Z. Zhu, Y. Yang, R. Ding, and Y. Li, "High-frequency electrical model of through-silicon vias for 3-D integrated circuits considering eddy current and proximity effects," *IEEE Trans. Compon., Packag., Manuf. Technol.*, vol. 7, no. 12, pp. 2036–2044, Sep. 2017, doi: [10.1109/TCPMT.2017.2741340](https://doi.org/10.1109/TCPMT.2017.2741340).
- [25] S. Hu, L. Wang, Y.-Z. Xiong, T. G. Lim, B. Zhang, J. Shi, and X. Yuan, "TSV technology for millimeter-wave and terahertz design and applications," *IEEE Trans. Compon., Packag., Manuf. Technol.*, vol. 1, no. 2, pp. 260–267, Feb. 2011, doi: [10.1109/TCPMT.2010.2099731](https://doi.org/10.1109/TCPMT.2010.2099731).
- [26] X. Liu, Z. Zhu, Y. Liu, Q. Lu, X. Yin, and Y. Yang, "Wideband substrate integrated waveguide bandpass filter based on 3-D ICs," *IEEE Trans. Compon., Packag., Manuf. Technol.*, vol. 9, no. 4, pp. 728–735, Apr. 2019, doi: [10.1109/TCPMT.2018.2878863](https://doi.org/10.1109/TCPMT.2018.2878863).
- [27] Y. X. Zhou, D. X. Qu, X. J. Zhong, K. Li, and J. D. Ye, "A dual-band bandpass filter constructed by using t junctions I/O structure," in *Proc. Int. Conf. Wireless Commun. Signal Process. (WCSP)*, Oct. 2015, pp. 1–3, doi: [10.1109/WCSP.2015.7341052](https://doi.org/10.1109/WCSP.2015.7341052).
- [28] M. J. Joshi and A. B. Nandgaonkar, "Third order wideband bandpass filter for ISM band using stepped and hairpin composite," in *Proc. Int. Conf. Adv. Comput., Commun. Informat. (ICACCI)*, Aug. 2015, pp. 1799–1802, doi: [10.1109/ICACCI.2015.7275876](https://doi.org/10.1109/ICACCI.2015.7275876).
- [29] W.-S. Zhao, J. Zheng, S. Chen, X. Wang, and G. Wang, "Transient analysis of through-silicon vias in floating silicon substrate," *IEEE Electromagn. Compat.*, vol. 59, no. 1, pp. 207–216, Feb. 2017, doi: [10.1109/TEMC.2016.2592181](https://doi.org/10.1109/TEMC.2016.2592181).
- [30] T. Sie King, A. T. Ying Ying, and S. Hieng Tiong, "A microstrip diplexer using folded hairpins," in *Proc. IEEE Int. RF Microw. Conf.*, Dec. 2011, pp. 226–229, doi: [10.1109/RFM.2011.6168735](https://doi.org/10.1109/RFM.2011.6168735).
- [31] K. Wang, S.-W. Wong, G.-H. Sun, Z. N. Chen, L. Zhu, and Q.-X. Chu, "Synthesis method for substrate-integrated waveguide bandpass filter with even-order Chebyshev response," *IEEE Trans. Compon., Packag., Manuf. Technol.*, vol. 6, no. 1, pp. 126–135, Jan. 2016, doi: [10.1109/TCPMT.2015.2502420](https://doi.org/10.1109/TCPMT.2015.2502420).
- [32] F. Wang, V. F. Pavlidis, and N. Yu, "Miniaturized SIW bandpass filter based on TSV technology for THz applications," *IEEE Trans. THz Sci. Technol.*, vol. 10, no. 4, pp. 423–426, Jul. 2020, doi: [10.1109/TTHZ.2020.2974091](https://doi.org/10.1109/TTHZ.2020.2974091).



LEI KE received the B.Sc. degree from Xi'an University of Technology, Xi'an, China, in 2019, where he is currently pursuing the M.Sc. degree. His research interests include 3-D hairpin filter and cross-coupled SIW filter based on through silicon-via (TSV).



XIANGKUN YIN received the M.S. and Ph.D. degrees in microelectronics and solid state electronics from Xidian University, Xi'an, China, in 2010 and 2017, respectively. He did his research at The University of Manchester, U.K., as a Visiting Scholar, from 2019 to 2020. He is currently a Lecturer with the School of Microelectronics, Xidian University. His current research interests include low-power circuits, 3-D ICs based on the through-silicon-vias, and high-performance RF/microwave circuits.



NINGMEI YU (Member, IEEE) received the B.Sc. degree from Xi'an University of Technology, in 1986, and the M.Sc. and Ph.D. degrees from Tohoku University, in 1996 and 1999, respectively. From 1999 to 2001, she was an IC Design Engineer with OKI Corporation, Japan. From 2008 to 2009, she was a Visiting Researcher with The University of Tokyo. She is currently a Professor with Xi'an University of Technology, the Leader of electronic science and technology, and the Ph.D. Tutor. She is the author of one book, more than 100 articles, and holds ten patents. She has presided over seven national and provincial-level projects of the NSFC, Shaanxi Provincial Natural Science Fund, the Ministry of Education Scholarship Fund, six international cooperation projects, and three enterprise cooperation projects. She has undertaken four teaching reform projects. Her main research interest includes VLSI design and technology.



FENGJUAN WANG (Member, IEEE) received the B.A. degree in applied physics from Hebei University, Baoding, China, in 2007, and the M.S. and Ph.D. degrees in microelectronics and solid-state electronics from Xidian University, Xi'an, China, in 2010 and 2014, respectively. She did her research at The University of Manchester, U.K., as a Visiting Scholar, from 2019 to 2020. She is currently an Associate Professor with the Department of Electric Engineering, School of Automation and Information Engineering, Xi'an University of Technology, Xi'an. Her research interests include through silicon-via (TSV)-based integrated passive device design, thermal management, and thermo-mechanical performance of 3-D integrated circuits (3-D ICs).



YUAN YANG received the B.S., M.S., and Ph.D. degrees from Xi'an University of Technology, China, in 1997, 2000, and 2004, respectively. From 2000 to 2004, she was a Lecturer. In 2005, she did her research at Kyushu University, Japan, as a Visiting Scholar. From 2004 to 2009, she was an Assistant Professor. Since 2009, she has been a Professor with the Electronics Department, Xi'an University of Technology. Her main research interests include digital-analog mixed integrated circuit design, the design of track circuit systems, gate drive and protection circuits of the high-power IGBT, and wide-bandgap semiconductors.

...